PROCEEDINGS OF THE INTERNATIONAL CONFERENCE
NANOMATERIALS: APPLICATIONS AND PROPERTIES
Vol. **2** No 2, 02PCN33(5pp) (2013)

Specific Interactions and Crystallization of Drug-Loaded Micelles in the System: Prednisolon/PAAm-*b*-PEO-*b*-PAAm Micellar Solutions

T.B. Zheltonozhskaya[1,*], S.V. Partsevskaya[1,†], D.O. Klymchuk[2,+], V.F. Gorchev[3]

[1] *Kiev National University of Taras Shevchenko, Faculty of Chemistry, Department of Macromolecular Chemistry, 60 Vladimirskaya St., 01033 Kiev, Ukraine*
[2] *Institute of Botany, National Academy of Sciences of Ukraine, 2 Tereschenkovskaya St., 01601 Kiev, Ukraine*
[3] *Institute of Biochemistry, National Academy of Sciences of Ukraine, 9 Leontovycha St., 01601 Kiev, Ukraine*

(Received 12 June 2013; published online 31 August 2013)

Encapsulaton of poorly soluble crystallizing drug prednisolone (PS) in micellar solutions of PAAm-*b*-PEO-*b*-PAAm triblock copolymer (TBC) based on chemically complementary poly(ethylene oxide) and polyacrylamide (M_{nPEO} = 6 kDa, M_{nPAAm} = 116 kDa) was studied by dynamic light scattering and transmission electron microscopy. The equilibrium mechanism of the encapsulation process and the effect of specific aggregation of PS-loaded micelles by their "coronas" that promoted the drug crystallization were established. The question about the presence of TBC micelles inside crystalline space was discussed.

Keywords: Triblock copolymer, Intramolecular polycomplex, Micelles, Prednisolone, Encapsulation.

PACS numbers: 61.46.Df, 62.23.St

1. INTRIDUCTION

Encapsulation of toxic and poorly soluble drugs into polymeric micelles opens a way to ensure long-term circulation and controlled release of drugs in the blood stream and to protect living organisms from too much poisoning [1-5]. Self-assembly of asymmetric block copolymers forming intramolecular polycomplexes (IntraPCs) is one of the simplest ways to create micellar drug carriers, which contain a complex "core", possess high binding capability with respect to toxic or poorly soluble drugs of hydrophilic and hydrophobic origin, and could not be destructed up to individual polymer components in any competitive processes taking place in living organisms [6-8]. Earlier, we studied micellization of asymmetric IntraPC-forming triblock copolymers (TBCs) based on poly(ethylene oxide) and polyacrylamide (PAAm-*b*-PEO-*b*-PAAm) and found the formation of "hairy-type" polymolecular micelles (PMM) and monomolecular ones (MMM), which were in fact separate IntraPCs [7,8]. Significant encapsulation of a crystalline drug prednisolon (PS) by these micelles led to appearance of unusual "snow-flakes-like" structures.

We represent here additional studies of PS binding with TBC micelles performed by dynamic light scattering and transmission electron microscopy to show the nature of "snow-flakes-like" structures and the role of TBC micelles in PS crystallization.

2. EXPERIMENTAL SECTION

2.1 Materials

TBC sample with M_{nPEO} = 6 kDa and M_{nPAAm} = 116 kDa was obtained by a matrix free-radical block copolymerization of acrylamide from "Merk" (Germany) with poly(ethylene glycol) from "Aldrich" (USA). Ammonium cerium (IV) nitrate from the last firm was used as initiator. Synthesis scheme and mechanism of the template block copolymerization were detail discussed earlier [6]. Using ^{1}H NMR spectroscopy as in the study [8], we confirmed a chemical structure of TBC and determined the molecular weights of PAAm blocks and whole macromolecules. A sample of commercial crystalline PS from "Sigma Aldrich" (USA) was used as model drug.

2.2 Composition preparation

We prepared the PS/TBC micelles compositions at the constant copolymer content (0.3 and 0.5 kg·m^{-3} in TEM and DLS studies consequently) and different concentrations of the drug. The selected TBC concentrations were higher than the critical micellization concentration (CMC = 0.09 kg·m^{-3}) but essentially less than that (0.1 kg·m^{-3}), which was applied to established the drug encapsulation degree [7, 8]. Moreover, the relative contents of PS/TBC mixtures in DLS studies (φ = 0.065 ÷ 0.39 mol$_{PS}$/unit$_{TBC}$) were less than values of φ = 0.42 and 0.60, at which a quick formation of the "snow-flakes-like" structures took place [7, 8]. A small portion of PS ethanol solution (10 v/%) we introduced into a large volume of TBC solution in a dusty-free deionized water at the blending. All measurements were performed in 24 h after mixing. The drug-free aqueous solutions of TBC and the copolymer-free aqueous/ethanol (90/10 v/v) solutions of PS were studied too.

2.3 Transmission electron microscopy (TEM)

Electronic images of the copolymer micelles and their compositions with PS were obtained with a JEM-1230 instrument ("JEOL", Japan) operating at an accelerating voltage of 90 kV. A very small drops (~1·10^{-4} cm^3) of TBC micellar solution or PS/TBC compositions with φ = 0.2 or 0.4 mol$_{PS}$/unit$_{TBC}$ were deposited in cop-

*zheltonozhskaya@ukr.net
†partsevskaya@ukr.net
+microscopy.botany@gmail.com

per grids coated with Formvar film and carbon and then were dried for ~1 min at 20°C. TEM images were recorded in one day after the sample preparation.

2.4 Dynamic light scattering (DLS)

For DLS experiments, a ZetsSizer 3 instrument ("Malvern", UK) with a He-Ne laser operating at $\lambda = 632.8$ nm was used. 10-12 parallel measurements of the autocorrelation function were carried out in every solution at T = 20°C. Analysis of the results was carried out using the monomodal distribution approach and CONTIN algorithm (PCS program: size mode v.1.61). The last one allowed obtaining the size distributions based on particle volumes that resulted in more precise values of the average diameters of scattering particles.

3. RESULTS AND DISCUSSION

It was shown earlier [7, 8] that TBC micellization in dilute aqueous solutions developed due to the primary formation of IntraPCs in individual TBC macromolecules (because of hydrogen bonding PAAm and PEO blocks) followed by segregation of hydrophobic bound parts of both the blocks in water medium. Taking into account highly asymmetric character of TBC blocks, we assumed the appearance of the "hairy-type" micelles of spherical shape.

3.1 Parameters of TBC micelles in water

Real view of TBC micelles could be observed in TEM images represented in Fig. 1 and in the studies [7, 8]. They demonstrated mainly spherical structures comprised common "core" and developed "corona", which diameters changed in the range from 80 to 240 nm. It is clear that these micellar structures belong to the polymolecular-type micelles (PMMs).

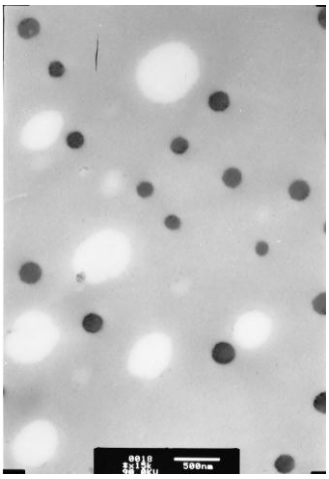

Fig. 1 – TEM image of polymolecular-type micelles of TBC

The image of TBC micelles represented in the study [8] showed additionally numerous dark points (or spots) with a size of 15 ÷ 30 nm and also some aggregates of large PMMs, which dimensions were higher than 240 nm. We attributed dark points in this image to separate IntraPCs, which form in fact the monomolecular-type micelles (MMMs) [9]. Here, we compare TEM results with the data of DLS studies, which were carried out in the drug-free TBC solutions (Fig. 2, Table 1).

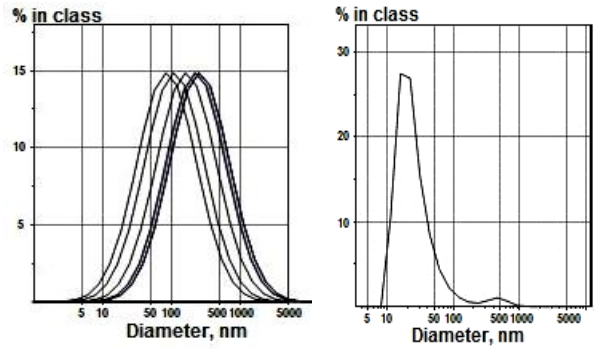

a b

Fig. 2 – Size distributions based on (**a**) scattered intensities and (**b**) particle volumes in TBC solution. $C_{TBC} = 0.3$ kg·m^{-3}

Table 1 – State of the copolymer micelles in aqueous solutions

System	d_{av} [1] nm	$d_{av(i)}$ [2] nm	$X_{(i)}$ [3] %	$d_{av(v)}$ [2] nm	$X_{(v)}$ [3] %	$d_{av(n)}$ [2] nm
TBC	109	218	100	28 468	97.1 2.9	18

[1] The average particle diameter based on the scattered intensities and monomodal distribution approach.
[3] The average diameters based on the scattered intensities, particle volume and particle number, consequently (CONTIN).
[4] The contributions of separate modes into the whole size distributions based on the scattered intensity and particle size.

A bimodal size distribution based on particle volume (Fig. 2 b), which was revealed by CONTIN processing, was the most important result. Due to this, the existence in TBC solution a large quantity (97.1 v/%) of small scattering particles (MMMs) with the average diameter $d_{av(v)} = 28$ nm and some quantity (2.9 v/%) of large scattering particles (PMMs and their aggregates) with $d_{av(v)} = 468$ nm (Table 1) was fully confirmed.

3.2 PS aggregation in water/ethanol solutions

DLS data in Table 2 reflect a state of PS molecules in water/ethanol (90/10 v/v) solutions at different drug concentrations. The bimodal size distributions based not only on particle volume but also on the scattered intensity were observed at the most concentrations of this poorly soluble drug excluding $C_{PS} = 0.274$ and partially 0.366 kg·m^{-3}. This meant that two kinds of aggregates with essentially different size existed in PS solutions. At the smallest PS concentration, the majority of drug molecules formed small aggregates with the average diameter $d_{av(v)} = 14$ nm (Table 2). It could be explained by a weak solubility of the drug in water/ethanol 90/10 v/v solutions (0.62 mg·cm^{-3}) [10]. At the increase in PS content up to 0.366 kg.$^{m-3}$, a size of small aggregates rose and their relative quantity diminished while the quantity and size of large aggregates grew. An opposite tendency was observed at further increase in PS content up to 0.55 kg.$^{m-3}$ (Table 2). Indeed, a size and relative quantity of small aggregates correspondingly decreased and rose, while both the parameters for large aggregates

diminished. We attributed such tendency to a partial precipitation of very large PS aggregates at $C_{PS} > 0.366$ kg·m^{-3} taking into account a very weak turbidity, which appeared in PS solutions with $C_{PS} = 0.458$ and 0.55 kg·m^{-3} in 24 hours' time. Thus, the conclusion about existence of a dynamic equilibrium between small and large PS aggregates in the given solvent has been achieved.

Table 2 – Prednisolon molecules in water/ethanol solutions1)

System	C, kg·m^{-3}	$d_{av(i)}$,2), nm	$X_{(i)}$, %	$d_{av(v)}$, nm	$X_{(v)}$, %	$d_{av(n)}$, nm
PS	0.092	42 1575	27.4 72.6	14 1828	98.1 1.9	10
	0.183	25 1002	5.4 94.6	18 1185	81.6 18.4	15
	0.274	2906	100	5968	99.9	46
	0.366	4076	100	40 7741	1.5 98.5	25
	0.458	41 4603	4.1 95.9	27 6166	20.2 79.8	24
	0.550	26 1600	5.4 94.6	19 1923	79 21	16

1)Ethanol content was equal to 10 v/%.

3.3 Encapsulation of PS and its consequences

The driving forces of PS encapsulation by TBC micelles such as hydrogen bonds and hydrophobic interactions were discussed in the previous works [7,8]. In this process, PAAm blocks more actively connected the drug molecules by both hydroxyl and carbonyl groups unlike PEO blocks. This meant that PS encapsulation developed mainly in TBC micellar "coronas", which contained the surplus (unbound with PEO) PAAm segments [8]. Such conclusion is very important to understand the results of DLS investigations of PS/TBC compositions (Fig. 3, Table 3). Note that all the compositions were transparent in the studied φ region in 24 hours' time.

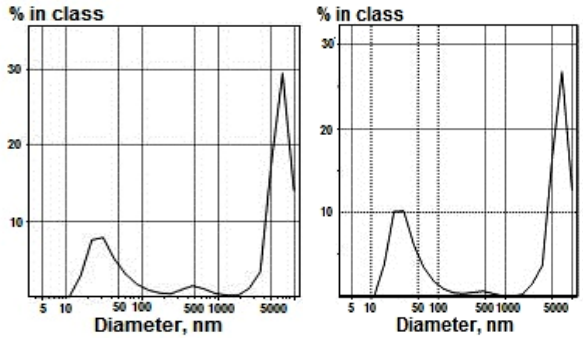

a b

Fig. 3 – The examples of size distributions based on particle volumes for PS/TBC compositions at φ = 0.065 (**a**) and 0.550 (**b**) $mol_{PS}/unit_{TBC}$. C_{TBC} = 0.3 kg·m^{-3}, T = 20°C.

For the first two compositions with φ = 0.092 and 0.183, the size distributions based on particle volumes comprised three modes corresponded to three types of scattering particles (Fig. 3a). Two of them with less dav(v) values in Table 3 could be attributed to the drug-containing MMMs and PMMs. The appearance of third-type scattering particles, which contribution and dimension decreased to zero at the φ growth up to 0.195, we explain by an equilibrium mechanism of the encapsulation process (the higher PS content, the higher binding with TBC micelles) and the existence of a real competition between PS encapsulation and aggregation. The values of dav(v) for the third-type scattering particles in Table 3, which are commensurable with those for large PS aggregates (Table 2), confirm this conclusion. When PS content had minimum value (φ = 0.065), the aggregation process strongly competed with the drug encapsulation. Due to this, free large PS aggregates could be identified in a solution. At the increasing PS content up to φ = 0.195, the drug encapsulation became predominant process. This led to a practical disappearance of large PS aggregates. Thus, a value of φ = 0.195 would correspond to a saturation of micelles by PS molecules.

In this context, the data of TEM (Fig. 4) are of special interest. They showed the presence as small as large micelles, which sizes were varied in the regions of 16 ÷ 200 and 470 ÷ 2400 nm (Fig. 4a, c). Also, they revealed the fact of strong aggregation of small and large drug-loaded micelles by their "coronas". Such aggregation actively developed at the composition drying (because initial PS/TBC solutions were transparent) and led to formation of PS crystals together with micelles (Fig. 4a, d).

Table 3 – The effect of PS encapsulation on TBC micelles

System	C_{PS}, kg·m^{-3}	φ, mol/unit	d_{av}, nm	$d_{av(i)}$, nm	$d_{av(v)}$, nm	$X_{(v)}$, %	$d_{av(n)}$, nm
PS/TBC	0.092	0.065	254	309 5743	43 601 6912	29.6 4.7 65.7	26
	0.183	0.130	163	443	39 567 1299	81.0 12.4 6.6	25
	0.274	0.195	85	30 496	16 670	96.7 3.3	12
	0.366	0.260	232	181 5306	37 6738	31.4 67.6	25
	0.550	0.390	255	198 5485	40 442 6815	37.0 1.8 61.2	26

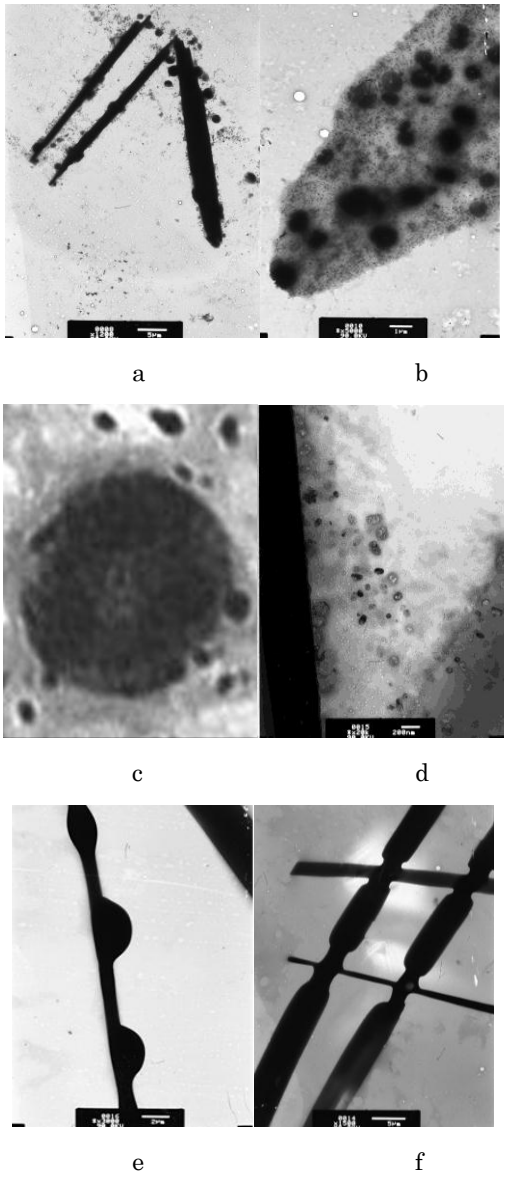

Fig. 4 – TEM images of: (a-d) specific aggregation and crystallization of PS-loaded micelles, (c) a large PS-loaded TBC micelle composed of numerous small ones, (a, d) PS crystals with micelles at their surface, and (e, f) unusual crystal morphology in PS/TBC compositions. $C_{TBC} = 0.5$ kg·m^{-3}; φ = 0.2 (a-e) and 0.4 (f) $mol_{PS}/unit_{TBC}$

This interesting fact could be explained by a preferential connection of the poorly soluble crystallizing PS with PAAm blocks in micellar "coronas". In this case, an important question about the presence of TBC micelles not only on a crystal surface (Fig. 4 a,d) but also inside crystal space appears. A strong increase in TEM images a, b showed a presence in the large mainly spherical micelles numerous small ones, which were connected with each other and formed a regulated fractal structure (Fig. 4**c**). This result allowed assuming that PS crystallization developed in the intermicellar space of these large aggregates at the composition drying and led to including small TBC micelles (in fact, the drug-loaded IntraPCs) inside crystals. The displaying unusual crystal morphology ((Fig. 4 e,f)), which is non-characteristic for the crystals of pure PS [11], may be a certain confirmation for such point of view. Thus, specific interactions of the PS-loaded TBC micelles promoted the drug crystallization.

A sharp increase in the scattered intensity of PS/TBC compositions and also the appearance of a third mode in the size distributions based on particle volumes took place at φ > 0.195 (Table 3). Such picture, namely, the formation of third-type scattering particles of a great size was explained by the strengthening of micelle aggregation due to participation of the surplus PS molecules non-connected with TBC micelles.

A separate attention would be focused on the changes in $d_{av(v)}$ values versus φ for the small drug-containing TBC micelles (Table 3). The increase in $d_{av(v)}$ from 28 nm (the average diameter of MMMs in water) to 43 nm at φ = 0.065 is replaced by a gradual reduction in the value up to 16 nm at φ = 0.195 followed by its growth to the number ~37 – 40 nm at further enhance in φ to 0.39. At first sight, such alterations could be attributed to the changes in the IntraPC state under influence of PS encapsulation (to swelling or contraction of IntraPCs). At the same time, the fact of the enhanced capability of the PS-loaded micelles to aggregation does not allow doing this. Moreover, the visible changes in morphology of small micelles (from spherical shape for MMMs in the solutions of pure TBC to preferentially spheroid one for small drug-loaded TBC micelles at φ = 0.2) was fixed at a strong magnification of images in Fig. 3 a-c.

4. CONCLUSION

It was established that TBC macromolecules formed the monomolecular-type and polymolecular-type micelles in dilute aqueous solutions. A strong aggregation of poorly soluble drug prednisolon in water/ethanol (90/10 v/v) solutions was also revealed. The small and large PS aggregates were in a dynamic equilibrium with each other. The micelles of TBC encapsulated PS in water/ethanol medium by equilibrium mechanism because of existence a real competition between the processes of drug encapsulation and aggregation. The drug encapsulation led to a strong specific aggregation of PS-loaded micelles by their "coronas" that was conditioned by the connection of drug molecules mainly with the "corona"-forming PAAm blocks. Two interesting phenomena such as the appearance of the large spherical PS-loaded copolymer micelles with fractal structure and also PS crystallization together with TBC micelles were considered as the results of this aggregation.

REFERENCES

1. G. Gaucher, M.-H. Dufresne, V.P. Sant, N. Kang, D. Maysinger, J.-C. Leroux, *J. Contr. Release* **109**, 169 (2005).
2. M. Motornov, Y. Roiter, I. Tokarev, S. Minko, *Prog. Polym. Sci.* **35**, 174 (2010).
3. Y. Ohya, A. Takahashi, K. Nagahama, *Adv. Polym. Sci.* **247**, 65 (2012).
4. A.C. Miller, A. Bershteyn, W. Tan, P.T. Hammond, R.E. Cohen, D.J. Irvine, *Biomacromolecules* **10**, 732 (2009).
5. K.Y. Dane, C. Nembrini, A.A. Tomei, J.K. Ehy, C.P. O'Neil, D. Velluto, M.A. Swartz, L. Inverandi, J.A. Hubbell, *J. Contr. Release* **156**, 154 (2011).
6. T. Zheltonozhskaya, N. Permyakova, L. Momot. In: *Hydrogen-Bonded Interpolymer Complexes: Formation, Structure and Applications* (New Jersey-London-Singapore etc.: World Scientific Publ. Co.: 2009).
7. T.B. Zheltonozhskaya, S.V. Partsevskaya, D.O. Klymchuk *J. Proc. Int. Conf. "Nanomaterials: Application and Properties"* **1**, No1, 01PCN05 (2012).
8. T. Zheltonozhskaya, S. Partsevskaya, S. Fedorchuk, D. Klymchuk, Yu. Gomza, N. Permyakova, L. Kunitskaya, *Europ. Polym. J.* **49**, 405 (2013).
9. K. Khougaz, Z. Gao, A. Eisenberg, *Macromolecules*, 27, 6341 (1994).
10. H.S.M. Ali, P. York, N. Blagden, S. Soitanpour, W.E. Acree, Jr Jouyban, A. Jouyban, *J. Chem. Eng. Data* **55**, 578 (2010).
11. X.-S. Li, J.-X. Wang, Z.-G. Shen, P.-Y. Zhang, J.-F. Chen, J. Yun, *Int. J. Pharm.* **342**, 26 (2007).